The Journal of Chemical Physics

RESEARCH ARTICLE | OCTOBER 26 2026

Microscopic relation between fictive temperature and fragility from configurational enthalpy fluctuations

Biman Bagchi

Check for updates

J. Chem. Phys. 165, 164506 (2026)
https://doi.org/10.1063/5.0344258

View Online
Export Citation

Articles You May Be Interested In

A model of heterogeneous undercooled liquid and glass accounting for temperature-dependent nonexponentiality and enthalpy fluctuation

J. Chem. Phys. (May 2024)

From fluctuating entropic neck to Rosenfeld–Adam–Gibbs crossover dynamics in supercooled liquids

J. Chem. Phys. (July 2026)

Revealing the connection between the slow β relaxation and sub-T_g enthalpy relaxation in metallic glasses

J. Appl. Phys. (December 2016)

31 October 2026 07:32:56

AIP Publishing

AIP Publishing
The Journal of Chemical Physics
Special Topics Open for Submissions
Learn More

The Journal of Chemical Physics ARTICLE pubs.aip.org/aip/jcp

Microscopic relation between fictive temperature and fragility from configurational enthalpy fluctuations

Cite as: J. Chem. Phys. 165, 164506 (2026); doi: 10.1063/5.0344258
Submitted: 18 May 2026 • Accepted: 6 October 2026 •
Published Online: 26 October 2026

View Online Export Citation CrossMark

Biman Bagchi[a)]

AFFILIATIONS

Solid State and Structural Chemistry Unit Indian Institute of Science, Bengaluru 560012, India

[a)]Author to whom correspondence should be addressed: profbiman@gmail.com

ABSTRACT

The fragility parameter m and the fictive temperature $T_f(t)$ are central quantities in the description of glass formation and structural arrest. Calorimetric studies have long established a connection between fragility, cooling rate, and the frozen fictive temperature. Here, we develop a microscopic dynamical basis for this connection by relating $T_f(t)$ to configurational enthalpy fluctuations. The delayed configurational enthalpy response is governed by the normalized enthalpy–enthalpy time-correlation function, which also determines the configurational part of the frequency-dependent heat capacity. The fictive temperature follows from this delayed enthalpy response, while fragility enters separately through the temperature dependence of the structural relaxation time and hence through the material-time clock. This separation leads to a general memory expression for the full time-dependent $T_f(t)$, with the familiar Tool equation emerging in the Debye limit. The formulation, therefore, distinguishes two roles: the enthalpy correlation function determines the relaxation kernel, whereas fragility determines how rapidly that kernel is traversed during cooling. The conventional cooling-rate dependence of the frozen fictive temperature then appears as a limiting consequence rather than the starting point of the theory. Quantitative prediction deep in the nonequilibrium glass requires a continuation of the structural clock to depend on both T and T_f.

Published under an exclusive license by AIP Publishing. https://doi.org/10.1063/5.0344258

31 October 2026 07:32:56

I. INTRODUCTION

The concept of fictive temperature, T_f, was introduced to characterize the nonequilibrium structural state of a glass that falls out of equilibrium during cooling.[1–3] Physically, T_f may be regarded as the temperature at which the instantaneous configurational state of the system would be in equilibrium. While the bath temperature $T(t)$ is externally controlled, the configurational degrees of freedom may become too slow to follow it. During cooling, the structure can, therefore, retain the characteristics of an earlier, higher-temperature state, so that $T_f(t) > T(t)$. The difference $T_f - T$ then provides a measure of structural departure from equilibrium, while the evolution of $T_f(t)$ reflects the progressive arrest of configurational motion as the structural relaxation time increases on approaching the glass transition.

A quantitative phenomenological description of this behavior was developed by Tool, Narayanaswamy, and Moynihan.[1–3] In the resulting Tool–Narayanaswamy–Moynihan (TNM) description, the relaxation time depends on both the instantaneous bath temperature and the structural state, represented by T_f. This framework has been remarkably successful in describing calorimetric cooling, heating, and aging experiments. The fictive temperature has subsequently become a useful state variable in discussions of vitrification, physical aging, and nonequilibrium relaxation in molecular, inorganic, and polymeric glasses.[4–7]

A particularly important development was the quantitative connection between fictive temperature and kinetic fragility established by Angell and co-workers. Velikov *et al.* showed, in the context of hyperquenched glasses, that strongly quenched states may possess fictive temperatures substantially above the conventional glass-transition temperature and used calorimetric recovery to characterize their kinetic state.[8] Wang *et al.* subsequently developed a direct differential-scanning calorimetry procedure in which the fictive temperatures of glasses prepared at different cooling rates were

Published under an exclusive license by AIP Publishing

used to determine kinetic fragility.[9] Thus, the connection among cooling or quench rate, frozen fictive temperature, and fragility is considerably stronger than the qualitative statement that rapid cooling causes the structure to fall out of equilibrium earlier. The rate dependence of the frozen T_f contains quantitative information about the temperature dependence of the structural relaxation time.[10–15]

The fragility parameter, m, introduced and developed extensively by Angell and co-workers, characterizes the steepness of the temperature dependence of the structural relaxation time near the glass transition.[16–18] It is conventionally defined by

$$m = \left. \frac{d \log_{10} \tau(T)}{d(T_g/T)} \right|_{T=T_g}, \tag{1}$$

where T_g is the operational glass-transition temperature and $\tau(T)$ is the structural relaxation time. Strong glass formers display a comparatively weak increase of τ on cooling, whereas fragile glass formers exhibit a much more rapid growth. The calorimetric work of Angell and co-workers, therefore, established an operational relation between preparation history, T_f, and m. In the specific sense relevant to the present work, however, this relation remains phenomenological: it identifies and quantifies the rate–T_f–fragility connection without specifying the microscopic fluctuation process responsible for the delayed configurational enthalpy response.

The TNM framework likewise represents the structural state through T_f and commonly introduces a nonlinearity parameter describing the relative influence of T and T_f on the relaxation time. Extensions based on the Adam–Gibbs relation and related thermodynamic approaches have provided additional insight into the dependence of relaxation on configurational entropy and preparation history.[19,20] Real glass-forming liquids also generally exhibit nonexponential relaxation, often represented by a stretched-exponential form, and empirical correlations among stretching, nonlinearity, and fragility have been discussed extensively.[21] These approaches demonstrate that the structural state and the kinetic slowing down are intimately linked, but they do not by themselves identify a unique microscopic time-correlation function from which the evolution of $T_f(t)$ can be constructed.

A more microscopic treatment of nonequilibrium glass relaxation was developed by Lubchenko and Wolynes within the random first-order transition (RFOT) framework.[22,23] Their aging theory treats the relaxation rate as depending on both the ambient temperature and a history-dependent structural state characterized by a fictive temperature and it relates the nonlinearity of nonequilibrium relaxation to the equilibrium liquid fragility. Subsequent work by Wolynes et al. extended this picture to spatially heterogeneous aging and rejuvenation, in which a local fictive-temperature field is coupled to a spatially varying mobility field.[24,25] These theories represent an important microscopic advance because they connect history dependence to activated rearrangements and spatially heterogeneous mobility rather than treating T_f solely as a phenomenological fitting variable.

At the same time, the microscopic origin of the activation barrier in glassy relaxation remains a nontrivial issue. RFOT expresses the barrier in terms of configurational entropy and an amorphous mismatch penalty, but the microscopic mechanical origin of this mismatch cost is not unique. In recent work, an alternative elasticity-based description has been developed in which activated relaxation arises from elastic heterogeneity, local soft regions, and non-affine deformation, providing a mechanical origin for a scale-dependent mismatch penalty without requiring the RFOT construction. The present work does not require a choice between these competing barrier descriptions. Our concern here is at a different, and experimentally more direct, level: the relation between the microscopic configurational enthalpy fluctuations, the calorimetric response, and the evolution of the fictive temperature.

This viewpoint is motivated by the fact that the slow configurational contribution to the frequency-dependent heat capacity is directly related to the configurational enthalpy–enthalpy time-correlation function.[26] The same correlation function, therefore, contains information about the delayed enthalpy response that gives rise to the fictive-temperature lag. This suggests a natural route to the problem: first determine the nonequilibrium configurational enthalpy response to a prescribed thermal history and then define $T_f(t)$ by mapping that instantaneous configurational enthalpy onto its equilibrium value at an effective temperature.

The issue addressed in the present work is, therefore, not whether fictive temperature and fragility are connected. That connection is well established by the calorimetric studies of Angell and co-workers, by TNM phenomenology, and by subsequent theories of aging. Our objective is more specific: to identify a microscopic time-domain object that generates the structural memory entering $T_f(t)$ and to determine separately how fragility controls the rate at which that memory is traversed during cooling.

The central distinction of the present formulation is that the configurational enthalpy–enthalpy time-correlation function determines the shape of the structural memory kernel, whereas fragility enters through the temperature dependence of the structural relaxation time and hence through the material-time clock. The fictive temperature is not introduced as an independent microscopic variable; rather, it follows from the delayed configurational enthalpy response. This leads naturally to the sequence,

$$C^*_{p,\mathrm{conf}}(\omega) \longrightarrow H_{\mathrm{conf}}(t) \longrightarrow T_f(t), \tag{2}$$

while the fragility enters through the structural clock,

$$m \longrightarrow \tau(T) \longrightarrow \zeta(t) \longrightarrow T_f(t). \tag{3}$$

Using linear response, we derive a general memory expression for the time-dependent fictive temperature in terms of the configurational enthalpy relaxation function. In the single-relaxation-time limit, the familiar Tool equation emerges naturally. We then show how the fragility parameter enters through the accumulated material time and how the conventional cooling-rate dependence of the frozen fictive temperature follows as a limiting consequence. Finally, the same formulation provides a frequency-domain interpretation: the temperature shift of the configurational heat-capacity loss peak is governed by the same structural clock that controls the evolution of $T_f(t)$. The resulting framework, therefore, connects microscopic enthalpy fluctuations, dynamic calorimetry, fictive-temperature evolution, and kinetic fragility within a single time-correlation description.

31 October 2026 07:32:56

Published under an exclusive license by AIP Publishing

II. FREQUENCY-DEPENDENT HEAT CAPACITY AND THE FICTIVE TEMPERATURE

We now derive the relation between the frequency-dependent heat capacity and the time-dependent fictive temperature. It is useful to clarify the logic of the construction at the outset. The frequency-dependent heat capacity is a response function of the slow configurational degrees of freedom and, in general, its spectrum depends on the instantaneous structural state of the material. At the same time, this response function determines how the configurational enthalpy follows an imposed temperature history. The fictive temperature is then obtained by mapping this nonequilibrium configurational enthalpy onto the equilibrium configurational enthalpy at an effective temperature. Thus, there is no circular definition: $C^*_{p,\mathrm{conf}}(\omega)$ determines the delayed enthalpy response, while $T_f(t)$ is the thermodynamic label assigned to that enthalpy. Equivalently, one may regard the mismatch $T_f(t) - T(t)$ as a measure of the unrelaxed configurational enthalpy, but the more direct route followed in the following is to compute the enthalpy response first and then define $T_f(t)$.

This construction is particularly useful because it identifies a single microscopic quantity—the configurational enthalpy–enthalpy correlation function—that underlies both the calorimetric response and the subsequent evolution of the fictive temperature.

The essential point is that the fictive temperature is not introduced as an independent dynamical variable. Rather, it is defined from the instantaneous configurational enthalpy. Thus, the logical order is

$$C^*_{p,\mathrm{conf}}(\omega) \longrightarrow H_{\mathrm{conf}}(t) \longrightarrow T_f(t). \tag{4}$$

At constant pressure, the total enthalpy may be separated into fast and slow contributions,

$$H(t) = H_{\mathrm{fast}}[T(t)] + H_{\mathrm{conf}}(t), \tag{5}$$

where H_{fast} contains rapidly equilibrating kinetic, vibrational, librational, and local contributions, while H_{conf} denotes the slowly relaxing configurational enthalpy. The fast part remains slaved to the instantaneous bath temperature,

$$H_{\mathrm{fast}}(t) = H^{\mathrm{eq}}_{\mathrm{fast}}[T(t)]. \tag{6}$$

The configurational part, however, may lag behind equilibrium during cooling or aging.

The corresponding heat capacity may be decomposed as

$$C_p^{\mathrm{eq}}(T) = C_p^{\mathrm{fast}}(T) + C_p^{\mathrm{conf}}(T), \tag{7}$$

with

$$C_p^{\mathrm{fast}}(T) = \frac{dH^{\mathrm{eq}}_{\mathrm{fast}}}{dT}, \qquad C_p^{\mathrm{conf}}(T) = \frac{dH^{\mathrm{eq}}_{\mathrm{conf}}}{dT}. \tag{8}$$

In dynamic calorimetry, this separation appears through the high- and low-frequency limits of the complex heat capacity,

$$C_p^{\infty}(T) = C_p^{\mathrm{fast}}(T), \qquad C_p^{0}(T) = C_p^{\mathrm{eq}}(T). \tag{9}$$

The configurational heat-capacity increment is, therefore,

$$\Delta C_p(T) = C_p^{0}(T) - C_p^{\infty}(T) = C_p^{\mathrm{conf}}(T). \tag{10}$$

Thus, the fast kinetic and vibrational part is not neglected; it is contained in C_p^{∞}. The slow part is relevant to glassy relaxation. We now transfer to the frequency-dependent description and the right-hand side of the above-mentioned equation gives

$$C^*_{p,\mathrm{conf}}(\omega; T) = C^*_p(\omega; T) - C_p^{\infty}(T). \tag{11}$$

Although $C^*_{p,\mathrm{conf}}(\omega; T)$ may itself depend on the structural state of the liquid, its role here is to determine the delayed configurational enthalpy response to an imposed bath-temperature history. The fictive temperature is then obtained by mapping this nonequilibrium configurational enthalpy onto the corresponding equilibrium configurational enthalpy. Thus, $T_f(t)$ is not an independent external field in the present derivation, but a thermodynamic label assigned to the unrelaxed enthalpy.

We next relate this quantity to the configurational enthalpy response. Consider an imposed bath-temperature history $T(t)$. In the linear-response regime, the configurational enthalpy responds to this thermal history with a delay. In the frequency domain, this response may be written as

$$\delta H_{\mathrm{conf}}(\omega) = C^*_{p,\mathrm{conf}}(\omega; T)\ \delta T(\omega), \tag{12}$$

where $\delta T(\omega)$ is the imposed bath-temperature perturbation. Importantly, the perturbing temperature in Eq. (12) is the bath temperature, not $T_f - T$. The fictive temperature will be introduced only after the configurational enthalpy has been obtained.

Following the dynamic heat-capacity formulation of Saito *et al.*,[26] the configurational part of the heat capacity is related to the normalized configurational enthalpy–enthalpy time-correlation function (EETCF), $\Phi_H(t;\ T)$, defined by

$$\Phi_H(t; T) = \frac{\langle \delta H_{\mathrm{conf}}(t)\delta H_{\mathrm{conf}}(0)\rangle_T}{\langle [\delta H_{\mathrm{conf}}(0)]^2\rangle_T}. \tag{13}$$

Using the above-mentioned definition, we can now write down the corresponding configurational heat capacity as[26]

$$C^*_{p,\mathrm{conf}}(\omega; T) = \Delta C_p(T)\big[1 - i\omega\hat{\Phi}_H(\omega; T)\big], \tag{14}$$

where

$$\hat{\Phi}_H(\omega; T) = \int_0^{\infty} dt\ e^{-i\omega t}\Phi_H(t; T). \tag{15}$$

Equation (14) contains the microscopic input: the slow heat-capacity spectrum is determined by the configurational enthalpy fluctuations.

The equivalent time-domain form follows by inverse transformation. Substituting the frequency-domain expression for $C^*_{p,\mathrm{conf}}(\omega)$ from Eq. (14) into the linear-response relation, Eq. (12), and then transforming back to the time domain yields a convolution expression for the configurational enthalpy. Physically, this convolution represents the delayed response of the configurational degrees of freedom to the imposed temperature history, with the relaxation kernel determined by the enthalpy–enthalpy correlation function. For a general temperature history, $T(t)$, the configurational enthalpy is

$$H_{\mathrm{conf}}(t) = H^{\mathrm{eq}}_{\mathrm{conf}}[T(t)] - \int_0^t ds\ \Delta C_p[T(s)]\ \Phi_H(t - s; T)\ \dot{T}(s). \tag{16}$$

31 October 2026 07:32:56

Published under an exclusive license by AIP Publishing

The first term is the enthalpy that would be obtained if the configurational degrees of freedom remained in equilibrium with the bath. The second term is the delayed response arising from the finite relaxation time of the slow structural modes.

We now define the fictive temperature. It is the equilibrium temperature at which the configurational enthalpy would have the instantaneous nonequilibrium value,

$$H_{\rm conf}(t) \equiv H^{\rm eq}_{\rm conf}[T_f(t)]. \tag{17}$$

Therefore,

$$H^{\rm eq}_{\rm conf}[T_f(t)] = H^{\rm eq}_{\rm conf}[T(t)] - \int_0^t ds\, \Delta C_p[T(s)]\, \Phi_H(t-s;T)\, \dot{T}(s). \tag{18}$$

This is the direct and desired relation between the configurational enthalpy response and the fictive temperature.

For small to moderate departures from equilibrium, we linearize $H^{\rm eq}_{\rm conf}[T_f(t)]$ about $T(t)$,

$$H^{\rm eq}_{\rm conf}[T_f(t)] \simeq H^{\rm eq}_{\rm conf}[T(t)] + \Delta C_p[T(t)]\,[T_f(t) - T(t)]. \tag{19}$$

We now substitute the above into Eq. (18), which gives

$$T_f(t) - T(t) = -\frac{1}{\Delta C_p[T(t)]} \int_0^t ds\, \Delta C_p[T(s)]\, \Phi_H(t-s;T)\, \dot{T}(s). \tag{20}$$

If the configurational heat-capacity increment varies only weakly over the temperature interval relevant to structural arrest, ΔC_p may be taken outside the integral, leading to cancellation between the numerator and denominator. This simplifies the above-mentioned expression to

$$T_f(t) = T(t) - \int_0^t ds\, \Phi_H(t-s;T)\, \dot{T}(s). \tag{21}$$

Equation (21) is the desired time-domain relation. It has been obtained in the order,

$$C^*_{p,\rm conf}(\omega) \to H_{\rm conf}(t) \to T_f(t)$$

and, therefore, avoids any circular use of T_f as the initial perturbation.

For a linear cooling protocol,

$$T(t) = T_0 - qt, \qquad q > 0, \tag{22}$$

so that $\dot{T} = -q$. Equation (21) becomes

$$T_f(t) = T(t) + q \int_0^t ds\, \Phi_H(t-s;T). \tag{23}$$

This form shows explicitly that the fictive temperature exceeds the bath temperature during cooling because the configurational enthalpy retains memory of earlier, higher-temperature states.

In a glass-forming liquid, the structural relaxation time changes strongly with temperature during cooling. As a result, equal intervals of laboratory time do not correspond to equal amounts of structural relaxation. At high temperature, where $\tau(T)$ is short, the structure evolves rapidly, whereas near the glass transition, the same interval of laboratory time produces only a very small amount of configurational relaxation. It is, therefore, convenient to introduce a reduced or material time that measures the accumulated progress of structural relaxation along the thermal history. Following the Tool–Narayanaswamy description of aging and later material-time formulations, we define the reduced time by

$$d\zeta = \frac{dt}{\tau[T(t)]}, \tag{24}$$

so that

$$\zeta(t) = \int_0^t \frac{dt'}{\tau[T(t')]}. \tag{25}$$

The reduced time, therefore, represents the total amount of configurational relaxation accumulated up to time t. When $\tau(T)$ becomes very large near the glass transition, the internal clock effectively slows down and $\zeta(t)$ increases only weakly even though laboratory time continues to advance.

The preceding convolution was written for a fixed reference temperature. During cooling, however, the relaxation spectrum itself shifts continuously because the structural relaxation time changes with temperature. To extend the convolution to a nonisothermal history, we adopt the standard reduced-time, or material-time, approximation used in TNM-type descriptions of structural relaxation. The assumption is not that the relaxation function is strictly temperature-independent in laboratory time, but rather that its shape is approximately invariant when expressed in terms of the accumulated internal time ζ.

Thus, the kernel is assumed to depend on the amount of structural relaxation elapsed between the earlier time s and the observation time t, rather than on the laboratory-time interval $t - s$ alone. This accumulated relaxation is measured by

$$\zeta(t) - \zeta(s) = \int_s^t \frac{du}{\tau[T(u)]}. \tag{26}$$

Consequently, the nonisothermal relaxation kernel is approximated as

$$\Phi_H(t-s;T) \to \Phi_H[\zeta(t) - \zeta(s)]. \tag{27}$$

This step is the usual thermorheological-simplicity assumption: cooling changes the rate at which the internal clock advances, but does not strongly change the shape of the normalized configurational enthalpy relaxation function. If the spectral shape itself changes appreciably with temperature, the present expression must be generalized by allowing Φ_H to depend explicitly on both temperature and structural state.

The fictive-temperature relation then becomes

$$T_f(t) = T(t) - \int_0^t ds\, \Phi_H[\zeta(t) - \zeta(s)]\, \dot{T}(s) \tag{28}$$

31 October 2026 07:32:56

Published under an exclusive license by AIP Publishing

or for linear cooling,

$$T_f(t) = T_0 - qt + q\int_0^t ds\, \Phi_H[\zeta(t) - \zeta(s)]. \tag{29}$$

A. Debye limit and emergence of the Tool equation

Finally, we consider the single-relaxation-time, or Debye, limit of the configurational enthalpy relaxation. In reduced time, this corresponds to

$$\Phi_H(\Delta\zeta) = \exp(-\Delta\zeta). \tag{30}$$

For a general thermal history, Eq. (28) may then be written as

$$T_f(t) = T(t) - \int_0^t ds\, \exp[-\zeta(t) + \zeta(s)]\, \dot{T}(s). \tag{31}$$

We define the lag variable,

$$y(t) = T_f(t) - T(t). \tag{32}$$

Then,

$$y(t) = -\int_0^t ds\, \exp[-\zeta(t) + \zeta(s)]\, \dot{T}(s). \tag{33}$$

Differentiating this expression with respect to t gives

$$\frac{dy}{dt} = -\dot{T}(t) - \frac{d\zeta}{dt}\, y(t). \tag{34}$$

Since

$$\frac{d\zeta}{dt} = \frac{1}{\tau[T(t)]}, \tag{35}$$

we obtain

$$\frac{dy}{dt} = -\dot{T}(t) - \frac{y(t)}{\tau[T(t)]}. \tag{36}$$

Using $y(t) = T_f(t) - T(t)$, so that

$$\frac{dy}{dt} = \frac{dT_f}{dt} - \dot{T}(t), \tag{37}$$

one finally obtains

$$\frac{dT_f}{dt} = \frac{T(t) - T_f(t)}{\tau[T(t)]}. \tag{38}$$

Thus, the usual Tool-type equation appears as the single-relaxation-time limit of the more general heat-capacity response formulation. The microscopic object remains the configurational enthalpy–enthalpy time-correlation function, or equivalently $C^*_{p,\mathrm{conf}}(\omega)$.

We next discuss the relation of fragility m with the enthalpy–enthalpy time correlation function (EETCF) defined above.

III. FRAGILITY AND THE TIME DEPENDENCE OF THE FICTIVE TEMPERATURE

We now connect the fictive-temperature dynamics developed above the fragility parameter m. The essential point is simple. The shape of the configurational enthalpy relaxation function is determined by the enthalpy–enthalpy time correlation function, or equivalently by the configurational part of the frequency-dependent heat capacity. Fragility enters through the temperature dependence of the structural relaxation time that sets the clock for this relaxation.

A. Fragility as the temperature dependence of the structural clock

The Angell fragility parameter is defined by

$$m = \left.\frac{d\log_{10}\tau(T)}{d(T_g/T)}\right|_{T=T_g}, \tag{39}$$

where T_g is the operational glass transition temperature and $\tau(T)$ is the structural relaxation time.

Near T_g, the most direct local representation consistent with this definition is

$$\log_{10}\tau(T) = \log_{10}\tau_g + m\left(\frac{T_g}{T} - 1\right), \tag{40}$$

where

$$\tau_g \equiv \tau(T_g). \tag{41}$$

Thus,

$$\tau(T) = \tau_g\, 10^{m\left(\frac{T_g}{T} - 1\right)}. \tag{42}$$

Equation (42) should not be viewed as a new global empirical law for the relaxation time. It is a local representation near T_g that inserts the experimentally defined fragility into the fictive-temperature dynamics. A VFT, parabolic, or Adam–Gibbs form may be used instead, provided that its slope at T_g gives the same value of m.

B. Reduced time and the general relation for $T_f(t)$

From the dynamic heat-capacity formulation of Sec. III A, the fictive-temperature trajectory may be written as

$$T_f(t) = T(t) - \int_0^t ds\, \Phi_H[\zeta(t) - \zeta(s)]\, \dot{T}(s), \tag{43}$$

where Φ_H is the normalized configurational enthalpy relaxation function. The reduced time is

$$\zeta(t) = \int_0^t \frac{dt'}{\tau[T(t')]}. \tag{44}$$

For clarity, we first write the result using a bath-temperature-dependent relaxation time. Additional dependence on T_f may be included in a TNM-like extension, but is not needed for the basic relation between fragility and fictive-temperature evolution.

31 October 2026 07:32:56

Published under an exclusive license by AIP Publishing

For a linear cooling protocol,

$$T(t) = T_0 - qt, \qquad q > 0, \tag{45}$$

one has $\dot{T} = -q$ and Eq. (43) becomes

$$T_f(t) = T_0 - qt + q\int_0^t ds\, \Phi_H[\zeta(t) - \zeta(s)]. \tag{46}$$

Substituting Eq. (42) into Eq. (44) gives

$$\zeta(t) - \zeta(s) = \int_s^t \frac{du}{\tau_g\, 10^{m\left(\frac{T_g}{T_0 - qu} - 1\right)}}. \tag{47}$$

Therefore,

$$T_f(t) = T_0 - qt + q\int_0^t ds\, \Phi_H\left[\int_s^t \frac{du}{\tau_g\, 10^{m\left(\frac{T_g}{T_0 - qu} - 1\right)}}\right]. \tag{48}$$

Equation (48) is the central time-domain result of this section. It shows that fragility affects $T_f(t)$ by controlling the rate at which reduced time accumulates during cooling. The microscopic relaxation function Φ_H is supplied by the configurational enthalpy TCF, while m sets the temperature dependence of the structural clock.

C. Debye limit

In the Debye limit, the heat-capacity formulation reduces to the local Tool-type equation derived in Sec. II A. Substituting the fragility representation of $\tau(T)$ into that equation gives

$$\frac{dT_f}{dt} = \frac{T(t) - T_f(t)}{\tau_g\, 10^{m(T_g/T(t) - 1)}}. \tag{49}$$

This equation is useful because it displays the role of fragility transparently. For a fragile liquid, $\tau(T)$ grows rapidly as T is lowered through the glass transition region. The denominator in Eq. (49), therefore, increases rapidly, and $T_f(t)$ ceases to follow the bath temperature. For a strong liquid, the growth of $\tau(T)$ is weaker, and the fictive temperature remains closer to equilibrium over a broader temperature range.

D. Near-T_g form

Near T_g,

$$\frac{T_g}{T} - 1 \simeq \frac{T_g - T}{T_g}. \tag{50}$$

Equation (42) then becomes

$$\tau(T) \simeq \tau_g\, \exp\left[\mu(T_g - T)\right], \qquad \mu = \frac{m \ln 10}{T_g}. \tag{51}$$

The parameter μ is the local thermal slope of the structural clock. It is directly proportional to fragility. Thus, a large value of m implies that the enthalpy relaxation spectrum shifts rapidly to low frequency as the temperature is lowered, causing earlier arrest of the configurational enthalpy and a larger fictive-temperature lag.

E. Physical interpretation

The result of this section can be summarized as follows: The configurational enthalpy TCF determines the relaxation function Φ_H. The frequency-dependent heat capacity measures the same relaxation spectrum. The fictive temperature is obtained by mapping the slow configurational enthalpy lag onto an equivalent equilibrium enthalpy. Fragility enters through the temperature dependence of the relaxation time or, equivalently, through the temperature shift of the calorimetric loss spectrum.

Thus,

$$\text{enthalpy TCF} \longrightarrow C^*_{p,\text{conf}}(\omega) \longrightarrow T_f(t), \tag{52}$$

while

$$m \longrightarrow \tau(T) \longrightarrow \zeta(t) \longrightarrow T_f(t). \tag{53}$$

This is the desired connection between fragility and fictive-temperature dynamics. Fragility does not change the basic microscopic origin of the response; it controls how rapidly the enthalpy relaxation spectrum shifts with temperature.

IV. FRAGILITY AND THE DEPARTURE OF $T_f(t)$ FROM $T(t)$

The preceding formulation allows a robust statement about the onset of nonequilibrium behavior during cooling. The Angell fragility parameter m is defined from the equilibrium, or metastable-equilibrium, supercooled liquid as T_g is approached from above. It, therefore, controls the temperature dependence of the structural relaxation time in the regime where the system is still able to equilibrate.

During cooling, the fictive temperature follows the bath temperature as long as the accumulated reduced time is large enough for configurational equilibration. Departure from equilibrium begins when the structural relaxation time becomes comparable with the timescale over which the bath temperature changes appreciably. Thus, the condition for the onset of a fictive-temperature lag may be written schematically as

$$\tau(T_{\text{on}}) \sim \frac{\Delta T}{q},$$

where $q = |dT/dt|$ is the cooling rate and ΔT is the temperature interval over which the relaxation time changes significantly. This criterion should be viewed as an onset condition, not as a precise prediction of the final frozen fictive temperature.

Using the local fragility representation near T_g,

$$\tau(T) \simeq \tau_g 10^{m(T_g/T - 1)},$$

one sees that a larger value of m produces a sharper increase in $\tau(T)$ upon cooling. Consequently, fragile liquids develop a fictive-temperature lag over a narrower temperature interval, whereas strong liquids remain closer to equilibrium over a broader interval.

Below T_g, however, the system is no longer in equilibrium at the bath temperature. The relaxation kernel governing further evolution of $T_f(t)$ cannot, in general, be identified with the equilibrium enthalpy–enthalpy correlation function at T. A quantitative prediction of the final frozen fictive temperature, therefore, requires a

31 October 2026 07:32:56

Published under an exclusive license by AIP Publishing

nonequilibrium continuation of the structural clock, for example, through a TNM-like relaxation time $\tau(T, T_f)$. The present theory should, therefore, be interpreted as giving a microscopic basis for the onset and growth of the fictive-temperature lag, rather than a fully quantitative formula for the final frozen value of T_f.

A. Definition of frozen fictive temperature

The frozen fictive temperature is defined as the asymptotic value of $T_f(t)$ after the system has fallen out of equilibrium during cooling,

$$T_f^{\mathrm{fr}}(q) \equiv \lim_{t\to\infty} T_f(t). \tag{54}$$

Physically, it corresponds to the temperature at which structural relaxation effectively ceases on the timescale set by the cooling rate.

Starting from the time-domain relation derived in Sec. II, the frozen fictive temperature is defined and controlled by the point at which the reduced time no longer accumulates appreciably during cooling.

Hence, the frozen fictive temperature is determined by the region where relaxation effectively stops, i.e., where reduced time ceases to accumulate.

B. Physical freezing criterion

A physically transparent approximation is obtained by noting that freezing occurs when the structural relaxation time becomes comparable with the inverse cooling rate,

$$\tau(T_f^{\mathrm{fr}}) \sim \frac{\Delta T}{q}, \tag{55}$$

where ΔT is the temperature over which the system must relax. This criterion follows directly from the memory formalism: when $\tau(T)$ grows rapidly, the accumulation of reduced time,

$$\zeta = \int dt/\tau(T),$$

becomes negligible, so the kernel Φ no longer evolves and the structure freezes.

C. Relation between T_f^{fr} and fragility

Using the fragility-based expression for the relaxation time,

$$\tau(T) = \tau_g\ 10^{\,m\left(\frac{T_g}{T}-1\right)}, \tag{56}$$

and substituting into the freezing condition Eq. (55), we obtain

$$\tau_g\ 10^{\,m\left(\frac{T_g}{T_f^{\mathrm{fr}}}-1\right)} = \frac{\Delta T}{q}. \tag{57}$$

Taking $\log_{10}$,

$$\log_{10}\left(\frac{\Delta T}{q\tau_g}\right) = m\left(\frac{T_g}{T_f^{\mathrm{fr}}} - 1\right). \tag{58}$$

Solving for T_f^{fr} gives the central result,

$$T_f^{\mathrm{fr}}(q) = \frac{T_g}{1 + \frac{1}{m}\log_{10}\left(\frac{\Delta T}{q\tau_g}\right)}. \tag{59}$$

This is a closed-form expression relating the frozen fictive temperature, cooling rate, and fragility.

D. Near-T_g linearized form

For small deviations from T_g, we expand

$$\frac{T_g}{T_f^{\mathrm{fr}}} - 1 \simeq \frac{T_g - T_f^{\mathrm{fr}}}{T_g}. \tag{60}$$

Substituting into the logarithmic relation yields

$$T_g - T_f^{\mathrm{fr}} \simeq \frac{T_g}{m}\log_{10}\left(\frac{\Delta T}{q\tau_g}\right). \tag{61}$$

Thus, we obtain

$$T_f^{\mathrm{fr}}(q) \simeq T_g - \frac{T_g}{m}\log_{10}\left(\frac{\Delta T}{q\tau_g}\right). \tag{62}$$

This shows that the shift of the fictive temperature with cooling rate is inversely proportional to fragility.

E. Connection to experiments

Equations (59) and (62) provide a direct connection to calorimetric measurements.

- A plot of T_f^{fr} vs $\log q$ yields a slope proportional to $1/m$.
- Fragile liquids (large m) show weaker dependence of T_f^{fr} on q.
- Strong liquids (small m) show a larger shift of T_f^{fr} with cooling rate.

Thus, the frozen fictive temperature serves as a direct experimental probe of fragility.

F. Microscopic interpretation

Within the present framework, the origin of this relation is clear.

The structural relaxation function Φ is determined by the configurational enthalpy–enthalpy correlation function. Fragility does not modify the shape of Φ, but controls the rate at which reduced time accumulates via $\tau(T)$.

A larger fragility implies a sharper growth of $\tau(T)$ below T_g, leading to earlier arrest of the dynamics and hence a higher frozen fictive temperature. The result provides a direct connection between nonequilibrium glass formation and equilibrium dynamic properties encoded in fragility.

V. CALORIMETRIC LOSS PEAK AND A FREQUENCY-DOMAIN INTERPRETATION OF FRAGILITY

The formulation developed above shows that the fictive-temperature dynamics and the calorimetric spectrum originate

31 October 2026 07:32:56

Published under an exclusive license by AIP Publishing

from the same configurational enthalpy relaxation. We now use this connection to obtain a frequency-domain expression for the fragility parameter and to clarify its interpretation in terms of the temperature evolution of the configurational enthalpy spectrum.

The configurational part of the complex heat capacity may be written as

$$C_p^*(\omega;T) = C_p^{\infty}(T) + \Delta C_p(T)\chi(\omega;T), \tag{63}$$

where C_p^{∞} is the fast high-frequency contribution, ΔC_p is the configurational heat-capacity increment, and $\chi(\omega;\ T)$ is the normalized structural susceptibility. If $\Phi(t;\ T)$ is the normalized configurational enthalpy relaxation function, then

$$\chi(\omega;T) = 1 - i\omega\hat{\Phi}(\omega;T), \tag{64}$$

and hence,

$$C_p''(\omega;T) = \Delta C_p(T)\ \omega\int_0^{\infty}\Phi(t;T)\sin(\omega t)\ dt. \tag{65}$$

Thus, the loss spectrum of the frequency-dependent heat capacity directly probes the same configurational enthalpy relaxation function that controls the fictive-temperature response. In this sense, the time-domain evolution of $T_f(t)$ and the frequency-domain calorimetric loss are two representations of the same underlying configurational dynamics.

Under thermorheological simplicity, the relaxation function depends on time only through the scaled variable $t/\tau(T)$,

$$\Phi(t;T) = \varphi\left(\frac{t}{\tau(T)}\right), \tag{66}$$

where φ is a temperature-independent master function. Substitution into Eq. (65) gives

$$C_p''(\omega;T) = \Delta C_p(T)\ \mathcal{F}[\omega\tau(T)], \tag{67}$$

with

$$\mathcal{F}(y) = y\int_0^{\infty}\varphi(x)\sin(yx)\ dx. \tag{68}$$

Therefore, apart from the overall amplitude $\Delta C_p(T)$, the temperature dependence of the position of the calorimetric loss peak is governed by the single product $\omega\tau(T)$. This is the frequency-domain counterpart of the material-time description introduced above: temperature changes the rate at which the structural clock advances, while the normalized spectral shape is assumed to remain approximately invariant.

Let $\omega_p(T)$ denote the frequency at which $C_p''(\omega;T)$ is maximum. The peak condition gives

$$\omega_p(T)\tau(T) = y_p, \tag{69}$$

where y_p is a dimensionless number determined only by the shape of the relaxation spectrum. For Debye relaxation, $y_p = 1$; for nonexponential relaxation, y_p differs from unity but remains independent of temperature if the normalized spectral shape is invariant. The important point is that the temperature dependence of $\omega_p(T)$ is then entirely determined by that of the structural relaxation time.

Using the local fragility representation,

$$\tau(T) = \tau_g\ 10^{m\left(\frac{T_g}{T}-1\right)}, \tag{70}$$

we obtain

$$\omega_p(T) = \frac{y_p}{\tau_g}10^{-m\left(\frac{T_g}{T}-1\right)}. \tag{71}$$

Equivalently,

$$\log_{10}\omega_p(T) = \log_{10}\left(\frac{y_p}{\tau_g}\right) - m\left(\frac{T_g}{T}-1\right). \tag{72}$$

Thus, in the neighborhood of T_g, the slope of $\log_{10}\omega_p$ vs T_g/T is $-m$.

This leads to the following frequency-domain relation:

$$m = -\left.\frac{d\log_{10}\omega_p}{d(T_g/T)}\right|_{T=T_g}. \tag{73}$$

Equation (73) is equivalent to the usual Angell definition in terms of $\tau(T)$, but it provides a different physical interpretation. Fragility may be viewed as a measure of how rapidly the configurational enthalpy relaxation spectrum shifts toward lower frequency as the temperature is reduced toward T_g. In the time domain, the same quantity controls the slowing of the material-time clock and, therefore, the growth of the lag between $T_f(t)$ and the bath temperature.

This result also clarifies the respective roles of the relaxation kernel and fragility. The normalized enthalpy–enthalpy time-correlation function determines the shape of the relaxation spectrum, while m determines the temperature dependence of the characteristic timescale on which that spectrum is traversed. Thus, within the thermorheologically simple regime, fragility does not by itself specify the form of the relaxation kernel. Rather, it specifies the rate at which the entire enthalpy-fluctuation spectrum is displaced along the frequency axis as the system is cooled. This is precisely the same separation that appears in the time-domain fictive-temperature relation, where Φ_H supplies the memory kernel and $\tau(T)$ determines the accumulated material time.

Experimental evidence supports this common-clock interpretation. Specific-heat spectroscopy measurements by Birge and Nagel on glycerol and propylene glycol showed that the calorimetric relaxation follows the same temperature-dependent structural timescale inferred from other dynamical measurements.[27] More recent measurements by Jakobsen *et al.* demonstrated that dielectric, mechanical, and longitudinal specific-heat loss-peak frequencies exhibit closely related temperature dependences over broad dynamic ranges, while differing in their absolute timescales by approximately constant factors.[28] Roed *et al.* further showed that such proportionality persists under changes of temperature and pressure in 5PPE.[29] These observations support the view that different linear-response functions can be governed by a common structural clock even though the corresponding susceptibilities and spectral amplitudes are probe-dependent. This conclusion is also consistent with the "inner-clock" perspective developed by Peredo-Ortiz *et al.*, in which

31 October 2026 07:32:56

Published under an exclusive license by AIP Publishing

different linear-response functions of a glass-forming liquid are controlled by using a common structural relaxation timescale.[30,31]

It is important to distinguish this frequency-domain result from an attempt to construct a universal experimental plot of ω_p over temperature ranges where direct calorimetric loss-peak measurements may not be available. The content in Eqs. (69)–(73) is local to the regime in which the fragility representation is valid and in which the spectral shape may be regarded as approximately temperature independent. No extrapolation to experimentally inaccessible frequencies is required for the argument. The result is instead a statement about the structural clock: whenever a well-defined configurational loss peak can be followed with temperature, its local shift rate near T_g contains the same fragility information as the conventional relaxation-time representation.

The frequency-domain formulation, therefore, provides a complementary view of the connection developed in the preceding sections. The fictive temperature describes the delayed configurational enthalpy in the time domain, while the calorimetric loss peak describes the same configurational relaxation in the frequency domain. Fragility enters both descriptions through the temperature dependence of the structural timescale. The resulting connection between enthalpy fluctuations, calorimetric response, material time, and fictive temperature is the central microscopic content of the present formulation.

VI. NUMERICAL ILLUSTRATION: SILICA AND ETHANOL

We now illustrate the consequences of the above-mentioned theory for the fictive-temperature trajectory during cooling. The purpose of this calculation is not to fit a specific experiment, but to show how the contrast between strong and fragile glass formers appears in $T_f(T)$.

We use representative material parameters for silica and ethanol. Silica is a canonical strong glass former with low fragility, while ethanol is a fragile molecular liquid. The values of T_g and m are taken from standard compilations of glass-forming liquids.[17,18] The relaxation time at the glass transition is taken to be $\tau_g = 100$ s, the usual calorimetric convention.

The relaxation time is represented locally near T_g as

$$\tau(T) = \tau_g \, 10^{m\left(\frac{T_g}{T}-1\right)}. \tag{74}$$

The fictive temperature is obtained by numerically integrating the Debye-limit equation derived in Sec. II A, using the relaxation time in Eq. (73).

Under the linear cooling protocol,

$$T(t) = T_0 - qt, \qquad q = 2 \text{ K/min}. \tag{75}$$

Both T and T_f are scaled by T_g so that systems with very different glass transition temperatures can be compared on the same plot.

Figure 1 shows the resulting fictive-temperature trajectories. At high reduced temperature, both systems remain close to equilibrium and follow the line $T_f = T$. Upon cooling, the relaxation time increases and the system can no longer equilibrate on the cooling timescale. The departure of T_f from T, therefore, marks the onset of nonequilibrium structural arrest.

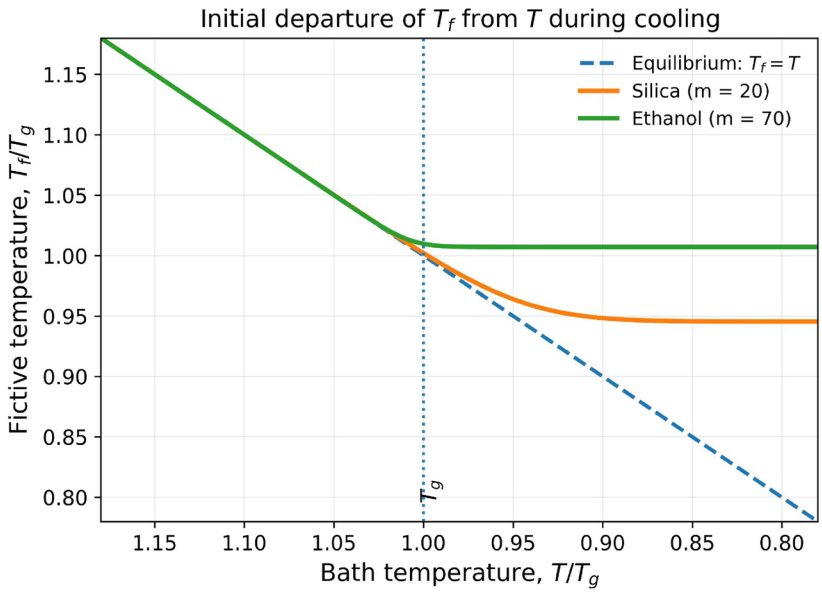


FIG. 1. Comparison of fictive-temperature evolution during linear cooling at rate $q = 2$ K/min for silica and ethanol, shown as T_f/T_g vs T/T_g. These two systems are chosen as representative limiting cases: silica is a canonical strong glass former, whereas ethanol is a fragile molecular glass former. The diagonal line denotes equilibrium, $T_f = T$. The results are obtained by integrating $dT_f/dt = [T(t) - T_f(t)]/\tau(T)$ with $\tau(T) = \tau_g \, 10^{m(T_g/T-1)}$ and $\tau_g = 100$ s. The parameters used are $T_g \simeq 1475$ K and $m \simeq 20$ for silica, and $T_g \simeq 97$ K and $m \simeq 70$ for ethanol, taken from standard compilations of glass-forming liquids and fragility data.[17,18,21] Silica remains close to equilibrium over a broad temperature range, whereas ethanol departs earlier and approaches a nearly constant fictive temperature, signaling structural arrest.

31 October 2026 07:32:56

Published under an exclusive license by AIP Publishing

TABLE I. Material parameters used in the numerical calculation of fictive-temperature trajectories. The values of T_g and m are representative literature values for silica and ethanol, respectively, while τ_g = 100 s is the conventional calorimetric definition of the glass transition.

Material	T_g (K)	Fragility m	τ_g (s)
Silica (SiO_2)	1475	~20	100
Ethanol	97	~70	100

The contrast between the two systems is direct. Silica, with low fragility, exhibits a gradual departure from equilibrium and remains close to the diagonal over a broad temperature interval. Ethanol, with much larger fragility, shows an earlier and sharper departure. At lower temperature, the ethanol curve approaches a nearly constant fictive temperature, corresponding to the regime $\tau(T) \gg 1/q$. This flattening is the dynamical signature of frozen configurational enthalpy.

The numerical comparison, therefore, illustrates the main physical conclusion: fragility controls how rapidly the enthalpy relaxation spectrum shifts to long times during cooling. A fragile liquid loses equilibrium over a narrower temperature interval and develops a larger fictive-temperature lag, while a strong liquid follows the bath temperature more closely.

The material properties of silica and ethanol used in this work are collected in Table I.

The material parameters employed in the present calculations are representative literature values widely used in discussions of glass-forming liquids and fragility. The fragility parameters and glass-transition temperatures for silica and ethanol were taken from standard compilations and reviews of glass-forming systems.[17,18,21] The purpose of the calculation is not to reproduce a specific calorimetric experiment quantitatively, but rather to illustrate how differences in fragility modify the fictive-temperature trajectory within the present theoretical framework.

Figure 1 provides a direct visualization of the freezing-out process in terms of the fictive temperature. At high temperatures, both systems follow the equilibrium line $T_f = T$, indicating that structural relaxation is fast compared to the cooling rate. As the temperature approaches T_g, the relaxation time increases rapidly and the system can no longer maintain equilibrium. This leads to a departure of T_f from T, marking the onset of nonequilibrium behavior. The effect is markedly different for strong and fragile liquids: silica, with low fragility, exhibits a gradual departure and remains close to equilibrium over a wide temperature range, whereas ethanol, with high fragility, shows an early and pronounced departure, followed by a rapid saturation of T_f. The flattening of the T_f curve at low temperatures corresponds to the regime where the structural relaxation time greatly exceeds the inverse cooling rate, $\tau(T) \gg 1/q$, and the configurational degrees of freedom are effectively frozen. This provides a clear dynamical interpretation of the frozen fictive temperature in terms of the arrest of enthalpy fluctuations.

The present formulation also complements recent fluctuation-based descriptions of glassy relaxation and nonequilibrium thermodynamics.[32]

VII. CONNECTION TO RFOT AGING AND ENERGY-LANDSCAPE DESCRIPTIONS

The present formulation also connects naturally with RFOT-based descriptions of aging in structural glasses. In RFOT theory, relaxation proceeds through activated rearrangements among metastable amorphous states, and the relaxation time is controlled by configurational entropy and mismatch penalties.[22,33] Extensions of RFOT to aging emphasize that a nonequilibrium glass is characterized not only by the bath temperature but also by a history-dependent structural state, often represented through a fictive temperature. Extensions of RFOT to nonequilibrium aging, rejuvenation, and mobility transport in glasses have been developed extensively by Wolynes and co-workers, emphasizing the role of history-dependent structural stability, activated rearrangements, and spatially heterogeneous mobility fields in aging dynamics.[23–25,34]

The perspective developed here is complementary. Instead of starting from an explicit landscape or mobility-field description, we formulate the problem in terms of the configurational enthalpy–enthalpy time-correlation function. The same correlation function determines the configurational part of the frequency-dependent heat capacity and the time evolution of the fictive temperature. Thus, the slow descent through the energy landscape during aging may be viewed, in the present formulation, as the progressive relaxation and spectral shift of configurational enthalpy fluctuations.

This connection suggests a direct bridge between RFOT aging theory and dynamic calorimetry. RFOT provides a physical picture of activated rearrangements and history-dependent stability, while the present theory provides an experimentally accessible representation in terms of $C_p^*(\omega)$, enthalpy fluctuations, and fictive-temperature dynamics. Fragility then enters through the temperature dependence of the structural relaxation clock common to both descriptions.

A more detailed incorporation of RFOT aging expressions for the relaxation time, including explicit configurational-entropy and spatial-heterogeneity effects, will be considered elsewhere.

VIII. CONCLUSION

In this work, we have developed a microscopic formulation that connects the fragility parameter m with the time evolution of the fictive temperature $T_f(t)$ during cooling. The connection is most direct and physically controlled in the regime where the system begins to fall out of equilibrium, that is, in the initial development of the lag between $T_f(t)$ and the bath temperature $T(t)$. This is the regime in which the equilibrium or metastable-supercooled-liquid relaxation spectrum near T_g still controls the loss of configurational equilibration.

The central starting point is a linear-response formulation in which the delayed configurational enthalpy response is governed by the configurational enthalpy–enthalpy time-correlation function. This same correlation function determines the configurational part of the frequency-dependent heat capacity. The fictive temperature is then obtained by mapping the nonequilibrium configurational enthalpy onto the corresponding equilibrium configurational enthalpy. Thus, the formulation naturally leads to a memory equation for $T_f(t)$, with the same structural relaxation kernel appearing in both dynamic calorimetry and fictive-temperature evolution.

31 October 2026 07:32:56

Published under an exclusive license by AIP Publishing

A key point is that the fragility parameter m is defined from the temperature dependence of the equilibrium structural relaxation time as T_g is approached from above. In the present theory, m, therefore, enters through the temperature dependence of the structural clock that controls the accumulation of reduced time during cooling. This clock determines when and how rapidly the fictive temperature begins to depart from the bath temperature. Below T_g, however, the system is no longer in equilibrium at the bath temperature and a quantitative description of the subsequent aging or the final frozen value of T_f requires a nonequilibrium continuation of the relaxation kernel, for example, of Tool–Narayanaswamy–Moynihan type.

Two principal results emerge from this formulation. First, we obtain a time-domain relation between the growth of the fictive-temperature lag and the structural relaxation kernel. In the Debye limit, this relation reduces to

$$\frac{dT_f}{dt} = \frac{T - T_f}{\tau(T, T_f)}, \tag{76}$$

where, near the onset of nonequilibrium behavior, the relaxation time may be approximated by its equilibrium supercooled-liquid form

$$\tau(T) \simeq \tau_g \, 10^{\,m\left(\frac{T_g}{T} - 1\right)}. \tag{77}$$

This result shows explicitly how fragility controls the initial rate at which $T_f(t)$ departs from $T(t)$ during cooling.

Second, we demonstrate that the temperature dependence of the calorimetric loss peak, $C_p''(\omega)$, is governed by the same structural clock. Under thermorheological simplicity,

$$\omega_p(T) \propto 10^{-m\left(\frac{T_g}{T} - 1\right)}, \tag{78}$$

so that the slope of $\log_{10} \omega_p$ vs T_g/T gives the same fragility parameter that is obtained from relaxation times. This establishes a direct connection between Angell fragility, the spectral shift of configurational enthalpy fluctuations, and the onset of fictive-temperature lag.

The theory provides a unified physical picture: fragility measures the rate at which the structural relaxation clock slows down upon cooling, which in turn controls the accumulation of reduced time and the eventual freezing of the configurational degrees of freedom. Within this framework, the shape of the relaxation function is determined by the microscopic enthalpy fluctuations, while fragility governs how rapidly this relaxation is traversed during cooling.

The predicted behavior is in agreement with experimental observations. Fragile liquids exhibit an early departure from equilibrium and a pronounced lag between T_f and T, leading to a higher frozen fictive temperature, while strong glass formers remain close to equilibrium over a wider temperature range. Similarly, the logarithmic dependence of T_f^{fr} on cooling rate and the temperature shift of the calorimetric loss peak are both consistent with calorimetric and dielectric measurements reported in the literature.

Therefore, the central new result of this work is the identification of fragility as a property encoded in the spectral evolution of enthalpy fluctuations. This provides a time-correlation-function-based interpretation of fragility, complementing and extending the traditional kinetic definition.

It is useful to emphasize the role of linear response in the present formulation. We have not treated $T_f(t) - T(t)$ as an externally imposed Kubo field. Instead, linear response enters through the experimentally measurable frequency-dependent heat capacity. The configurational part of $C_p^*(\omega)$ determines the delayed enthalpy response to a prescribed thermal history, and the fictive temperature is then obtained by mapping this nonequilibrium enthalpy onto the corresponding equilibrium configurational enthalpy. Thus, the response function is used in its calorimetric sense, while $T_f(t) - T(t)$ appears as the thermodynamic measure of the resulting enthalpy lag.

The present approach is also connected to earlier work in which the frequency-dependent heat capacity was obtained from microscopic theories of enthalpy fluctuations, including mode-coupling-type and memory-function descriptions. In this sense, the present theory may be viewed as using $C_p^*(\omega)$ as the bridge between microscopic enthalpy dynamics and the macroscopic fictive-temperature description.

Several limitations of the present formulation should be kept in mind. First, the derivation assumes a near-linear response regime, so that the mapping between the configurational enthalpy lag and $T_f(t) - T(t)$ can be linearized. Second, the use of reduced time assumes thermorheological simplicity: the relaxation spectrum may shift strongly with temperature, but its normalized shape is assumed not to change appreciably. This approximation can fail in systems with pronounced dynamic heterogeneity, multiple relaxation channels, strong secondary relaxations, crystallization, phase separation, or large structural changes during aging. Third, the Debye-limit equation used for numerical illustration is only the simplest limit of the more general convolution relation; quantitative description of real materials may require stretched-exponential or distributed relaxation kernels.

The numerical figures presented here should, therefore, be interpreted as illustrations of the central physical mechanism rather than as detailed fits to particular calorimetric protocols. More quantitative applications would require experimentally measured $C_p^*(\omega, T)$ over the relevant temperature range, including the temperature dependence of ΔC_p, possible changes in the spectral shape, and, when necessary, explicit dependence of the relaxation time on both T and T_f in the spirit of TNM theory.

In this sense, the experimentally established relation between cooling rate, fictive temperature, and fragility emerges here as a macroscopic consequence of an underlying microscopic memory dynamics governed by configurational enthalpy fluctuations.

The present work thus provides a direct and quantitative bridge between nonequilibrium glass formation and equilibrium dynamic properties encoded in fragility. The formulation opens the way to further developments, including extensions beyond the Debye limit, incorporation of nonexponential relaxation, and application to specific systems where the configurational heat capacity and relaxation spectra can be independently measured.

31 October 2026 07:32:56

Published under an exclusive license by AIP Publishing

AUTHOR DECLARATIONS

Conflict of Interest

The author has no conflicts to disclose.

Author Contributions

Biman Bagchi: Conceptualization (equal); Data curation (equal); Formal analysis (equal); Funding acquisition (equal); Investigation (equal); Methodology (equal); Project administration (equal); Software (equal); Validation (equal); Visualization (equal); Writing – original draft (equal); Writing – review & editing (equal).

DATA AVAILABILITY

The data that support the findings of this study are available within the article.

REFERENCES

[1] A. Q. Tool, J. Am. Ceram. Soc. **29**, 240 (1946).
[2] O. S. Narayanaswamy, J. Am. Ceram. Soc. **54**, 491 (1971).
[3] C. T. Moynihan, A. J. Easteal, M. A. DeBolt, and J. Tucker, J. Am. Ceram. Soc. **59**, 12–16 (1976).
[4] J. C. Mauro, R. J. Loucks, and P. K. Gupta, "Fictive temperature and the glassy state," J. Am. Ceram. Soc. **92**, 75–86 (2009).
[5] D. Cangialosi, V. M. Boucher, A. Alegría, and J. Colmenero, "Physical aging in polymers and polymer nanocomposites: Recent results and open questions," Soft Matter **9**(36), 8619–8630 (2013).
[6] T. Hecksher, N. B. Olsen, K. Niss, and J. C. Dyre, "Physical aging of molecular glasses studied by a device allowing for rapid thermal equilibration," J. Chem. Phys. **133**(17), 174514 (2010).
[7] D. Cangialosi, "Physical aging and vitrification in polymers and other glasses: Complex behavior and size effects," J. Polym. Sci. **62**, 1952–1974 (2024).
[8] V. Velikov, S. Borick, and C. A. Angell, "The glass transition of water, based on hyperquenching experiments," Science **294**, 2335–2338 (2001).
[9] L.-M. Wang, V. Velikov, and C. A. Angell, "Direct determination of kinetic fragility indices of glassforming liquids by differential scanning calorimetry: Kinetic versus thermodynamic fragilities," J. Chem. Phys. **117**, 10184–10192 (2002).
[10] Y. Yue *et al.*, J. Chem. Phys. **120**, 8053 (2004).
[11] R. Richert, "Dynamics of glass-forming liquids. XIV. A search for ultraslow dielectric relaxation in glycerol," J. Chem. Phys. **133**(7), 074502 (2010).
[12] M. D. Ediger, "Spatially heterogeneous dynamics in supercooled liquids," Annu. Rev. Phys. Chem. **51**, 99 (2000).
[13] N. O. Birge, "Specific-heat spectroscopy of glycerol and propylene glycol near the glass transition," Phys. Rev. B **34**, 1631–1642 (1986).
[14] C. M. Roland and R. Casalini, "Enthalpy relaxation and fragility in polychlorinated biphenyls," J. Therm. Anal. Calorim. **83**, 87–90 (2006).
[15] F. Spieckermann, D. Şopu, V. Soprunyuk *et al.*, "Structure-dynamics relationships in cryogenically deformed bulk metallic glass," Nat. Commun. **13**, 127 (2022).
[16] C. A. Angell, "Relaxation in liquids, polymers and plastic crystals — strong/fragile patterns and problems," J. Non-Cryst. Solids **131–133**, 13–31 (1991).
[17] C. A. Angell, Science **267**, 1924 (1995).
[18] M. D. Ediger, C. A. Angell, and S. R. Nagel, J. Phys. Chem. **100**, 13200 (1996).
[19] G. Adam and J. H. Gibbs, "On the temperature dependence of cooperative relaxation properties in glass-forming liquids," J. Chem. Phys. **43**, 139 (1965).
[20] I. M. Hodge, "Adam-Gibbs formulation of enthalpy relaxation near the glass transition," J. Res. Natl. Inst. Stand. Technol. **102**, 195 (1997).
[21] K. L. Ngai, *Relaxation and Diffusion in Complex Systems* (Springer, 2011).
[22] V. Lubchenko and P. G. Wolynes, "Theory of structural glasses and supercooled liquids," Annu. Rev. Phys. Chem. **58**, 235 (2007).
[23] V. Lubchenko and P. G. Wolynes, "Theory of aging in structural glasses," J. Chem. Phys. **121**, 2852 (2004).
[24] P. G. Wolynes, "Spatiotemporal structures in aging and rejuvenating glasses," Proc. Natl. Acad. Sci. U. S. A. **106**, 1353–1358 (2009).
[25] A. Wisitsorasak and P. G. Wolynes, "Fluctuating mobility generation and transport in glasses," Phys. Rev. E **88**, 022308 (2013).
[26] S. Saito, I. Ohmine, and B. Bagchi, "Frequency dependence of specific heat in supercooled liquid water and emergence of correlated dynamics," J. Chem. Phys. **138**, 094503 (2013).
[27] N. O. Birge and S. R. Nagel, "Specific-heat spectroscopy of the glass transition," Phys. Rev. Lett. **54**, 2674 (1985); N. O. Birge, Phys. Rev. B **34**, 1631 (1986).
[28] B. Jakobsen, T. Hecksher, T. Christensen, N. B. Olsen, J. C. Dyre, and K. Niss, "Identical temperature dependence of the time scales of several linear-response functions of two glass-forming liquids," J. Chem. Phys. **136**, 081102 (2012).
[29] L. A. Roed, K. Niss, and B. Jakobsen, "Communication: High pressure specific heat spectroscopy reveals simple relaxation behavior of glass forming molecular liquid," J. Chem. Phys. **143**, 221101 (2015).
[30] R. Peredo-Ortiz, M. Medina-Noyola, T. Voigtmann, and L. F. Elizondo-Aguilera, "'Inner clocks' of glass-forming liquids," J. Chem. Phys. **156**, 244506 (2022).
[31] J. C. Dyre, "Solid-that-flows picture of glass-forming liquids," J. Phys. Chem. Lett. **15**, 1603–1617 (2024).
[32] B. Bagchi, "Fictive temperature of a glassy system in terms of frequency-dependent specific heat: A memory function approach," Phys. Chem. Chem. Phys. **28**, 7913–7921 (2026).
[33] T. R. Kirkpatrick, D. Thirumalai, and P. G. Wolynes, "Scaling concepts for the dynamics of viscous liquids near an ideal glassy state," Phys. Rev. A **40**, 1045 (1989).
[34] V. Lubchenko and P. G. Wolynes, "Aging, jamming, and the limits of stability of amorphous solids," J. Phys. Chem. B **122**, 3280 (2018).

31 October 2026 07:32:56

Published under an exclusive license by AIP Publishing